
TEXT-TO-DECISION AGENT: LEARNING GENERALIST POLICIES FROM NATURAL LANGUAGE SUPERVISION

A PREPRINT

Shilin Zhang¹ Zican Hu¹ Wenhao Wu¹ Xinyi Xie² Jianxiang Tang¹
 Chunlin Chen¹ Daoyi Dong³ Yu Cheng⁴ Zhenhong Sun³ Zhi Wang¹

{shilinzhang, zicanhu, wenhaowu, jianxiangtang}@smail.nju.edu.cn xinyi_xie@email.ncu.edu.cn
 {clchen, zhiwang}@nju.edu.cn chengyu@cse.cuhk.edu.hk
 {zhenhong.sun, daoyi.dong}@anu.edu.au

¹ Department of Control Science and Intelligent Engineering, Nanjing University

² School of Information Engineering, Nanchang University

³ School of Engineering, Australian National University

⁴ Department of Computer Science and Engineering, The Chinese University of Hong Kong

ABSTRACT

RL systems usually tackle generalization by inferring task beliefs from high-quality samples or warmup explorations. The restricted form limits their generality and usability since these supervision signals are expensive and even infeasible to acquire in advance for unseen tasks. Learning directly from the raw text about decision tasks is a promising alternative to leverage a much broader source of supervision. In the paper, we propose Text-to-Decision Agent (T2DA), a simple and scalable framework that supervises generalist policy learning with natural language. We first introduce a generalized world model to encode multi-task decision data into a dynamics-aware embedding space. Then, inspired by CLIP, we predict which textual description goes with which decision embedding, effectively bridging their semantic gap via contrastive language-decision pre-training and aligning the text embeddings to comprehend the environment dynamics. After training the text-conditioned generalist policy, the agent can directly realize zero-shot text-to-decision generation in response to language instructions. Comprehensive experiments on MuJoCo and Meta-World benchmarks show that T2DA facilitates high-capacity zero-shot generalization and outperforms various types of baselines.

1 Introduction

Reinforcement learning (RL) has emerged as an effective mechanism for training autonomous agents to perform complex tasks in interactive environments [1, 2], unleashing its potential across frontier problems including preference optimization [3], diffusion model training [4], and reasoning like in OpenAI o1 and DeepSeek-R1 [5]. Despite its achievements, one of the grand challenges is *generalization*: building a general-purpose agent capable of handling multiple tasks in response to diverse user commands [6]. Current RL algorithms are usually specialized to a narrowly defined task distribution and struggle with poor generalization to unseen tasks, due to distribution shift and the lack of self-supervised pre-training techniques [7]. Recent studies usually rely on high-quality samples [8] or warmup explorations [9] to infer task-specific information for generalization at test time, while these supervision signals are expensive and even infeasible to acquire in advance for unseen tasks [10]. *This inspires us to explore a much broader source of supervision.*

Recently, large language models (LLMs), pre-trained on extensive text corpora, can encode a wealth of semantic knowledge with remarkable representation power and transferability [11]. The typical “text-to-text” interface enables task-agnostic architectures to achieve broad generalization with minimal or no domain-specific data [12]. The availability of large-scale text collections for aggregate supervision during model pre-training has revolutionized the

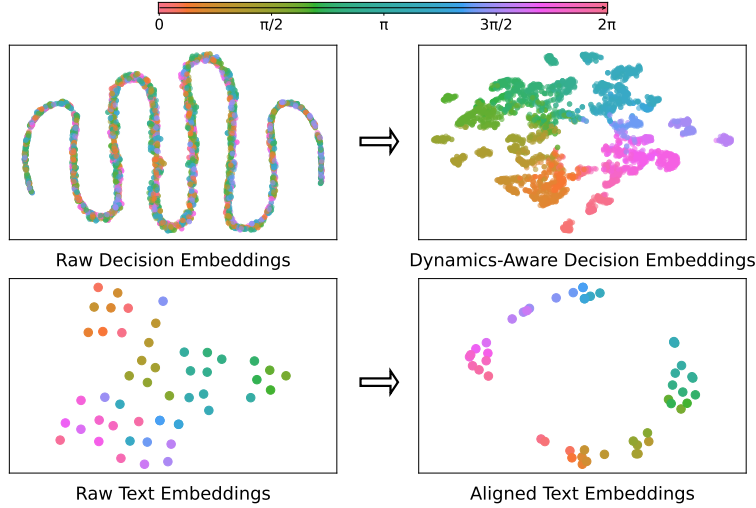


Figure 1: t-SNE visualization of Ant-Dir where tasks with target directions in $[0, 2\pi]$ are mapped to rainbow-colored points. Top: we encode multi-task data into dynamics-aware decision embeddings to capture task-specific environment dynamics. Bottom: we bridge the semantic gap between text and decision via contrastive pre-training. The aligned text embeddings follow a cyclic spectrum that exactly matches the periodicity of angular directions *in a physical sense*. This interesting finding shows that we effectively align text embeddings to comprehend environment dynamics and facilitate convincing language grounding in decision domains.

language and multi-modal communities in recent years [13]. Naturally, the above advancements highlight a promising question: *Could scalable pre-training methods that learn perception from the supervision embedded in natural language lead to a similar leap forward in developing generalist agents in RL?*

RL typically learns from active interactions with the outer world tied to specific environment dynamics, with unique decision-level representation distinct from the unbounded perception-level representation of natural language [14]. Recent studies facilitate language grounding to decision domains from various aspects, such as LLMs as policies [15, 16], LLMs as rewards [17, 18], and language-conditioned policy learning [19, 20]. Despite these efforts, how to harness unbounded representations of natural language knowledge for building generalist decision agents remains the following challenges: i) LLMs, trained on text corpora, typically lack grounding in the physical world and fail to capture any environment dynamics; ii) Leveraging LLMs for decision-making is prone to knowledge misalignment due to the semantic gap between the text and decision modalities; iii) Scalable implementations are necessary to fully harness language knowledge to train generalist decision models.

To tackle these challenges, we propose Text-to-Decision Agent (T2DA), a simple and scalable pre-training framework for learning generalist policies via aligning language knowledge with environment dynamics of decision tasks. First, we pre-train a generalized world model to encode multi-task data into dynamics-aware decision embeddings, effectively capturing task-specific environment dynamics. Second, inspired by CLIP [12], we predict which textual description goes with which decision embedding, efficiently bridging their semantic gap via contrastive language-decision pre-training. It distills the world model structure to the text modality and aligns text embeddings to comprehend the environment dynamics. Finally, we deploy T2DA on two mainstream conditional generation architectures, training generalist policies conditioned on aligned text embeddings. During evaluation, natural language is used to reference learned decision perceptions or describe new ones, and the agent can directly realize zero-shot text-to-decision generation according to textual instructions at hand. Extensive experiments show that T2DA transfers nontrivially to downstream tasks, achieves high-capacity zero-shot generalization, and outperforms various types of baselines.

In summary, our main contributions are as follows:

- We present a generalized world model designed to capture the environment dynamics, facilitating knowledge grounding in the physical world.
- We introduce contrastive language-decision pre-training to bridge their semantic gap, aligning the text embeddings to comprehend the environment dynamics.

- We propose a simple and scalable framework that learns generalist policies from natural language supervision, and develop scalable implementations with the potential to train decision models at scale: Text-to-Decision Diffuser and Text-to-Decision Transformer.

2 Related Work

Generalization in RL. Learning generalist policies is a long-standing challenge in RL. Early methods tackle this from the meta-learning perspective, which is differentiated into the optimization-based meta-RL such as MAML [21] and MACAW [22], and context-based meta-RL like PEARL [23], VariBAD [24], CORRO [25], CSRO [9], and UNICORN [26]. Recent studies of in-context RL attempt to leverage the in-context learning capability of transformer architectures to improve RL’s generalization via casting RL as an across-episodic sequential prediction problem with few-shot prompting at test time [27, 28], such as AD [29] and DPT [30]. In general, the above approaches rely on high-quality samples or domain knowledge to infer task beliefs during evaluation, which limits their generality with this restricted form of supervision. This inspires us to explore a much broader source of supervision from natural language.

LLMs for RL. Existing studies on leveraging knowledge of LLMs for RL domains can be categorized into three main threads: LLMs as policies, LLMs as rewards, and language-conditioned policy learning. The first kind directly utilizes LLMs, or vision-language models (VLMs), as the policy model [15, 31] or high-level semantic planner [14]. Most of them focus on tasks with text-only interactions, i.e., performing textual commands given textual observations [32, 33]. Otherwise, additional modules are needed to map the textual command into actions of other modalities [14, 16]. The second kind uses LLMs or VLMs to automate the generation and shaping of reward functions [17, 18, 34, 35] or state representations [36], providing denser information to facilitate RL training. The above studies usually focus on the single-task setting, while we aim to harness LLM knowledge towards generalist policy learning.

Language-conditioned policy. We focus on the third kind that learns a language-conditioned contextual policy, extracting the world knowledge encoded in LLMs to help train generalist decision agents. Previous studies attempt to translate the language to latent embeddings using pre-trained LLMs like BERT and GPT [37], while these embeddings are learned independently from decision tasks and may fail to capture task-related information. Early methods develop rule-based [38] or domain-specific [39] intermediate representations to capture task-related semantics, which could require a laborious design and lack scalability. BC-Z [19] trains a vision-based robotic manipulation system to achieve zero-shot generalization via conditioning an imitation learning policy on pre-trained embeddings of natural language. To improve language grounding, Pang et al. [40] translates natural language to task language via designing a referential game, and Pang et al. [20] uses supervised fine-tuning to enable bidirectional translation between language-described skills and rollout data. Overall, the challenges mainly include the inability to capture environment dynamics, knowledge misalignment due to semantic gaps, and limited model scalability. In the paper, we tackle these challenges to fully harness LLMs for building generalist decision models.

3 Method

In this section, we present Text-to-Decision Agent (T2DA), a simple and scalable framework to train generalist policies via effectively grounding natural language supervision with environment dynamics of decision tasks. Figure 2 illustrates the overall pipeline, followed by detailed implementations in the subsequent subsections. Corresponding algorithm pseudocodes are given in Appendix A.

3.1 Problem Statement

We consider a language-conditioned multi-task offline RL setting. Tasks follow a distribution $M_k = \langle \mathcal{S}, \mathcal{A}, \mathcal{T}_k, \mathcal{R}_k, \gamma \rangle \sim P(M)$, sharing the same state-action spaces while varying in the reward and state transition functions, i.e., environment dynamics. For each training task k , our system receives a user-provided natural language supervision l_k that describes the task (e.g., open the door), paired with an offline dataset $\mathcal{D}_k = \sum_i (s_i^k, a_i^k, r_i^k, s_i^{\prime k})$ collected by arbitrary behavior policies. The agent can only access the offline datasets $\sum_k (l_k, \mathcal{D}_k)$ to train a generalist policy $\pi(a|s, l)$ to follow language instructions. At test time, natural language is used to reference learned decision perceptions or describe new ones. The agent can perform text-to-decision generation in test environments in a zero-shot manner, given any language instruction l_{new} at hand. The primary objective is to obtain a highly generalizable policy that achieves strong zero-shot performance on unseen tasks.

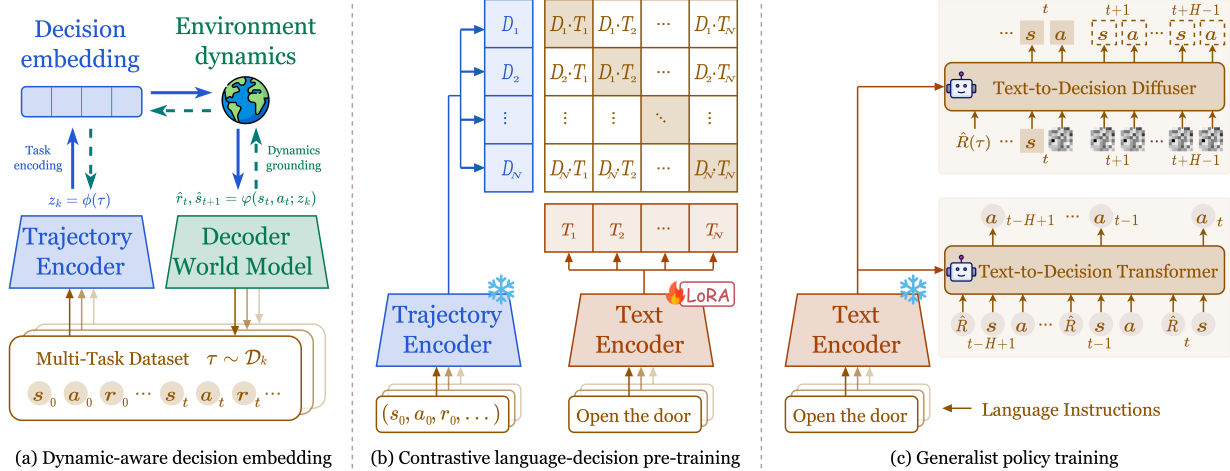


Figure 2: The overall pipeline of T2DA. (a) We encode the multi-task trajectories into dynamics-aware decision embeddings and decode the generalized world model conditioned on that embedding, effectively capturing the environment dynamics. (b) We bridge the semantic gap between decision and text by fine-tuning the text encoder (initialized from popular language models such as CLIP or T5) to align the produced text embeddings with dynamics-aware decision embeddings using contrastive loss. It distills the world model structure from decision embeddings to the text modality, aligning text embeddings to comprehend the environment dynamics. (c) We condition the generalist policy on the aligned text embeddings, and develop scalable implementations with the potential to train decision models at scale: Text-to-Decision Diffuser and Text-to-Decision Transformer. During evaluation, the agent can directly realize zero-shot text-to-decision generation according to textual instructions at hand, enabling high-capacity zero-shot generalization to downstream tasks.

3.2 Dynamics-Aware Decision Embedding

Natural language is a complex and unbounded representation of human instruction, and training policies to harness language supervision is nontrivial. A standard approach is to convert language instructions to simpler latent embeddings using popular pre-trained language models that can draw on a wealth of knowledge learned from copious amounts of text. However, directly applying these models to decision domains could fail to solve user-specific problems, as they are typically learned independently of decision-making tasks. A major challenge is that LLMs trained on text corpora typically lack grounding in the physical world and fail to capture any environment dynamics.

For effective grounding in decision domains, the agent ought to comprehend the environment dynamics of underlying tasks. RL typically learns from active interactions with the outer environment. The world model, i.e., the reward and state transition functions $p(s', r | s, a)$, fully characterizes the environment and presents a promising alternative to capturing the environment dynamics of decision tasks. Therefore, we introduce a generalized world model to encode the decision data from different tasks into a dynamics-aware embedding space. We separate the reasoning about the world model into two parts: i) encoding the dynamics-specific information into a latent embedding, and ii) decoding the environment dynamics conditioned on that embedding.

First, we use a trajectory encoder ϕ to abstract multi-task decision trajectories into a compact embedding z that captures task-specific dynamics. Specifically, we “tokenize” different elements (i.e., state, action, and reward) in the raw trajectory sequence $\tau = (s_0, a_0, r_0, \dots, s_L, a_L, r_L) \sim \mathcal{D}_k$, by lifting them to a common representation space as

$$e_t^s = f_\phi^s(s_t), e_t^a = f_\phi^a(a_t), e_t^r = f_\phi^r(r_t), \quad \forall t \in [0, L], \quad (1)$$

where $f_\phi^s, f_\phi^a, f_\phi^r$ are element-specific tokenizers. We arrange the tokens in a 1-D sequence of length $3 \times L$ as

$$\tau_e = (e_0^s, e_0^a, e_0^r, \dots, e_L^s, e_L^a, e_L^r). \quad (2)$$

Then, we utilize a bi-directional transformer E_ϕ to extract the dynamics-aware embedding from the input sequence of tokens as $z_k = E_\phi(\tau_e)$. The bi-directional structure allows for implicitly capturing the forward and inverse dynamics.

Second, we introduce a decoder φ containing a reward model \mathcal{R}_φ and state transition model \mathcal{T}_φ . The latent embedding is augmented into the input to predict the instant reward $\hat{r}_t = \mathcal{R}_\varphi(s_t, a_t; z_k)$ and next state $\hat{s}_{t+1} = \mathcal{T}_\varphi(s_t, a_t; z_k)$. The encoder-decoder pipeline is jointly trained by minimizing the reward and state transition prediction error conditioned

on the dynamics-aware decision embedding as

$$\mathcal{L}(\phi, \varphi) = \mathbb{E}_{\tau \sim \mathcal{D}_k} \left[\mathbb{E}_{z_k \sim \phi(\tau)} \left[\mathbb{E}_t \left[(r_t - \mathcal{R}_\varphi(s_t, a_t; z_k))^2 + (s_{t+1} - \mathcal{T}_\varphi(s_t, a_t; z_k))^2 \right] \right] \right], \quad \forall k. \quad (3)$$

In practice, we randomly sample a trajectory from the dataset as $\tau \sim \mathcal{D}_k$ and use its decision embedding to decode the dynamics of other trajectories in the same dataset as $\tau^* \in \mathcal{D}_k \setminus \tau$. The reason is that, since the embedding has access to the entire trajectory’s information, using it to decode the same trajectory can lead to deceptive traps during training. After proper training, the trajectory encoder is frozen for the subsequent learning phases.

3.3 Contrastive Language-Decision Pre-training

To successfully instruct generalist training with human language, we must bridge the semantic gap between text and the “decision modality”. Inspired by CLIP [12], we predict which textual description goes with which training task, bridging their semantic gap via contrastive learning. The core idea is to connect the language supervision with corresponding decision embeddings, distilling the world model structure to the text modality and aligning text embeddings to comprehend the environment dynamics.

Formally, given a batch of N (trajectory τ , textual task description l) pairs, we attempt to predict which of the $N \times N$ possible (trajectory, text) pairings across a batch actually occurred. We use the pre-trained trajectory encoder in Sec. 3.2 to extract the dynamics-aware decision embedding from the trajectory as $z = \phi(\tau)$. The text encoder is a transformer-based model ψ that could be initialized from one of a wide variety of popular language models such as CLIP [12] or T5 [41]. Then, the text embedding z_T is easily derived by tokenizing the textual instruction l and feeding it to the encoder as $z_T = \psi(l)$.

We model the pre-training task as a text-decision multi-modal learning problem by fine-tuning the text encoder while keeping the trajectory encoder fixed. The objective is to maximize the cosine similarity of the decision and text embeddings of the N real pairs in the batch while minimizing the cosine similarity of the embeddings of the $N^2 - N$ incorrect pairings. The symmetric similarities between the two modalities measured by cosine distance are defined as

$$\begin{aligned} \text{sim}(\tau, l) &= \exp(\alpha) \cdot \frac{\phi(\tau)W_D \cdot \psi(l)W_T}{\|\phi(\tau)W_D\| \cdot \|\psi(l)W_T\|}, \\ \text{sim}(l, \tau) &= \exp(\alpha) \cdot \frac{\psi(l)W_T \cdot \phi(\tau)W_D}{\|\psi(l)W_T\| \cdot \|\phi(\tau)W_D\|}, \end{aligned} \quad (4)$$

where α is a learnable temperature parameter that controls the range of similarities, and W_D and W_T are learnable projections that map feature representations of each modality to a joint multi-modal embedding space. Then, the decision-to-text $p(\tau)$ and text-to-decision $p(l)$ similarity scores in the batch are calculated as

$$p(\tau_k) = \frac{e^{\text{sim}(\tau_k, l_k)}}{\sum_{i=1}^N e^{\text{sim}(\tau_i, l_i)}}, \quad p(l_k) = \frac{e^{\text{sim}(l_k, \tau_k)}}{\sum_{i=1}^N e^{\text{sim}(l_i, \tau_i)}}. \quad (5)$$

Let $q(\tau)$ and $q(l)$ denote the ground-truth similarity scores where negative pairs have a probability of 0 and positive pairs have 1. We optimize a symmetric cross-entropy loss over these similarity scores as

$$\mathcal{L}(\psi) = \frac{1}{2} \mathbb{E}_{\tau, l} [\text{CE}(p(\tau), q(\tau)) + \text{CE}(p(l), q(l))], \quad (6)$$

where CE is the cross-entropy between two distributions. To effectively adapt the text encoder to the semantics of decision modality at a lightweight computing cost, we employ low-rank adaptation (LoRA) [42] to fine-tune the text encoder with the above contrastive loss. Experiments in Appendix F present the analysis of its efficiency and superiority compared to full-parameter fine-tuning.

This alignment process distills the environment dynamics from the decision embedding to the text modality. The aligned text embeddings not only serve as mere linguistic representations but also establish stronger comprehension of underlying decision tasks, effectively bridging the semantic gap between language supervision and decision dynamics.

3.4 Generalist Policy Learning

A widely adopted manner to tackle generalization in RL domains is to condition the policy on some representation that can capture task-relevant information, such as context-based meta-learning [23, 24] and prompt-based methods [8, 10].

Under this unified framework, we formulate the generalist agent as a task-conditioned policy model. There exists a true variable that represents the identity of the underlying task. Since we do not have access to this ground-truth information, we use a latent representation h to approximate that variable. Then, a base policy $\pi(\cdot, h)$ can be shared across tasks by conditioning on the task representation as

$$\pi_k(a | s) = \pi(a | s, h_k), \quad \forall k. \quad (7)$$

Previous studies usually approximate the task representation by acquiring expert decision data [8] or exploring the unseen task first [9]. This restricted form of supervision limits their universality and practicability since expensive high-quality samples or explorations are needed to specify any new task.

Motivated by the recent success of language models, we study a promising alternative that leverages a much broader source of supervision. Natural language is a flexible representation for transferring a variety of human ideas and intentions. Learning from its supervision could not only enhance the representation power but also enable efficient zero-shot transfer. We map the user-provided textual description of the task l to a latent embedding $\psi(l)$ via the fine-tuned text encoder in Sec. 3.3, and use this contextual embedding to approximate the task representation as $h \approx \psi(l)$. Then, the task-agnostic generalist policy is approximated by

$$\pi(a | s, h_k) \approx \pi(a | s, \psi(l_k)), \quad \forall k. \quad (8)$$

At test time, the agent can directly perform text-to-decision policy generation according to any textual instruction l_{new} at hand, enabling high-capacity zero-shot generalization to downstream tasks without the need for expensive decision demonstrations or warmup explorations.

3.5 Scalable Implementations

We develop scalable implementations of T2DA using two mainstream conditional generation architectures that hold the promise to train RL models at scale: the decision diffuser [43] and the decision transformer [44], yielding the following T2DA variants.

Text-to-Decision Diffuser (T2DA-D). Inspired by the recent success of text-to-image diffusion models [45, 46], we implement the text-to-decision counterpart by modeling the policy as a return-conditioned diffusion model with action planning. For model simplicity and scalability, we choose to diffuse over the H -step state-action trajectory as

$$x_c(\tau) = \begin{bmatrix} s_t & s_{t+1} & \dots & s_{t+H-1} \\ a_t & a_{t+1} & \dots & a_{t+H-1} \end{bmatrix}_c, \quad (9)$$

where c denotes the timestep in the forward diffusion process, and $c = 0$ corresponds to the unperturbed data.¹ To enable a generalist policy with natural language supervision, we include the fine-tuned text embedding $\psi(l)$ as an additional condition to the diffusion model. To this end, the generalist policy training is formulated as the standard problem of conditional generative modeling as

$$\max_{\theta} \mathbb{E}_{\tau \sim \mathcal{D}} \left[\log p_{\theta} \left(x_0(\tau) | \hat{R}(\tau), \psi(l) \right) \right], \quad (10)$$

where θ denotes diffusion parameters and \hat{R} is the return-to-go. The goal is learning to generate portions of a trajectory $x_0(\tau)$ from the task-specific condition $\psi(l)$ via estimating the conditional data distribution with p_{θ} . More details can be referred to as in Algorithms 3 and 5 in Appendix A.

4 Experiments

We comprehensively evaluate and analyze our method on popular benchmarking domains across datasets of varying qualities, aiming to answer the following research questions:

- Can T2DA achieve consistent performance gain on zero-shot generalization capacity to unseen tasks? We compare it to various types of strong baselines including offline meta-RL, in-context RL, and language-conditioned policy learning approaches. (Sec. 4.1)
- What is the contribution of each component to T2DA’s performance? We ablate both the T2DA-D and T2DA-T architectures to analyze the respective impact of world model pre-training, contrastive language-decision pre-training, and language supervision. (Sec. 4.2)

¹Decision diffuser diffuses over only states and trains another inverse dynamics model to generate actions. In contrast, we only keep a unified diffusion model to i) ensure simplicity with a single end-to-end model in a multi-task setting, and ii) unlock the potential of diffusion models at scale, rather than depending on additional MLPs to generate part of the information.

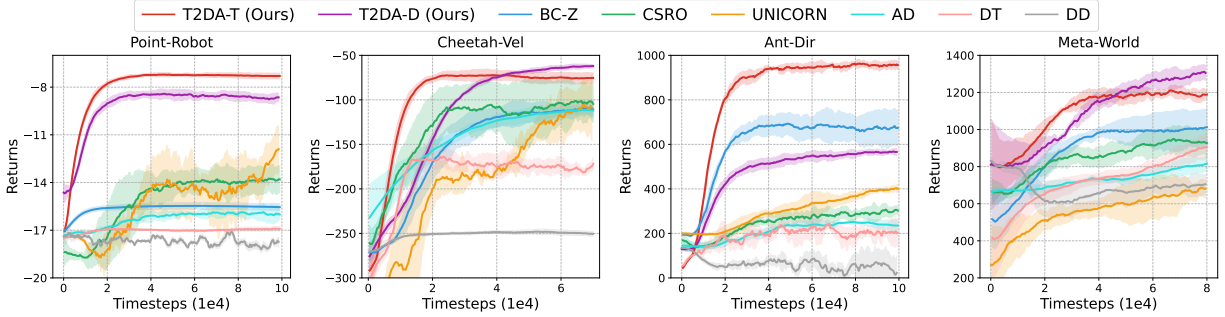


Figure 3: Zero-shot test return curves of T2DA against baselines using Mixed datasets.

Table 1: Zero-shot test returns of T2DA against baselines using Mixed datasets, i.e., numerical results of converged performance from Figure 3. Best results in **bold** and second best underlined.

Environment	T2DA-T	T2DA-D	BC-Z	CSRO	UNICORN	AD	DD	DT
Point-Robot	-7.2 \pm 0.1	<u>-8.4</u> \pm 0.2	-15.5 \pm 0.2	-13.7 \pm 0.5	-11.4 \pm 1.3	-15.8 \pm 0.2	-16.7 \pm 0.2	-16.9 \pm 0.2
Cheetah-Vel	-70.3 \pm 3.8	<u>-60.4</u> \pm 1.8	-107.4 \pm 8.5	-92.6 \pm 5.9	-94.1 \pm 20.0	-107.6 \pm 2.3	-247.7 \pm 2.9	-147.6 \pm 11.6
Ant-Dir	970.3 \pm 8.7	<u>570.6</u> \pm 13.1	<u>700.0</u> \pm 43.3	317.1 \pm 27.6	407.3 \pm 21.6	268.9 \pm 3.4	135.4 \pm 9.1	261.8 \pm 13.7
Meta-World	1274.5 \pm 48.4	<u>1376.4</u> \pm 39.6	1053.8 \pm 33.8	1005.2 \pm 69.6	754.6 \pm 62.7	921.0 \pm 66.9	831.8 \pm 14.0	970.4 \pm 60.5

- How robust is T2DA across diverse settings? We evaluate T2DA against baselines using offline datasets of varying qualities, and assess T2DA’s performance when initializing the text encoder from different LLMs. (Sec. 4.3)

Environments. We evaluate T2DA on three benchmarks that are widely adopted to assess generalization capacities of RL algorithms: i) the 2D navigation *Point-Robot*; ii) the multi-task MuJoCo locomotion control, containing *Cheetah-Vel* and *Ant-Dir*; and iii) the *Meta-World* manipulation platform, where a robotic arm is designed to perform a wide range of manipulation tasks, such as close faucet, lock door, open door, and press button. For each domain, we randomly sample a distribution of tasks captioned with text descriptions, and split them into training and test sets. We employ SAC [47] to independently train a single-task policy on each training task for offline dataset collection. We develop three types of offline datasets: *Mixed*, *Medium*, and *Expert*, following the common practice in offline RL [48]. Appendix B presents more details of environments and datasets.

Baselines. We compare T2DA to four competitive baselines that cover three representative paradigms in tackling RL generalization: the context-based offline meta-RL approaches, including 1) CSRO [9] and 2) UNICORN [26]; the in-context RL method of 3) AD [29]; and the language-conditioned policy learning method of 4) BC-Z [19]. Additionally, we include the base algorithms of T2DA implementations as two intuitive baselines: 5) DD [43] and 6) DT [44]. Appendix C gives more details.

For evaluation, all experiments are conducted using five different random seeds. The mean of received return is plotted as the bold line, with 95% bootstrapped confidence intervals of the mean indicated by the shaded region. Appendix D gives detailed implementations of T2DA, Appendix E shows tabular results for Sec. 4.2 and Sec. 4.3, and Appendix F gives analysis on fine-tuning of the text encoder.

4.1 Main Results

We compare our method against various baselines under an aligned zero-shot setting. Figure 3 and Table 1 present test return curves and numerical results of converged performance on various benchmark environments using *Mixed* datasets. A noteworthy point is that BC-Z generally achieves better performance than offline meta-RL and in-context RL baselines, especially in harder environments like *Ant-Dir* and *Meta-World*. This again validates our motivation of exploring a much broader source of supervision from natural language, harnessing the representation power and knowledge transferability embodied in LLMs.

In these diversified environments, both T2DA-D and T2DA-T consistently achieve significantly superior performance regarding learning speed and final asymptotic results compared to the three types of baselines. In most cases, T2DA-D and T2DA-T take the top two rankings for the best and second-best performance, and showcase comparably strong zero-shot generalization capacities on average across all evaluated environments. It highlights the effectiveness of both T2DA implementations using the two mainstream conditional generation architectures. Furthermore, our method typ-

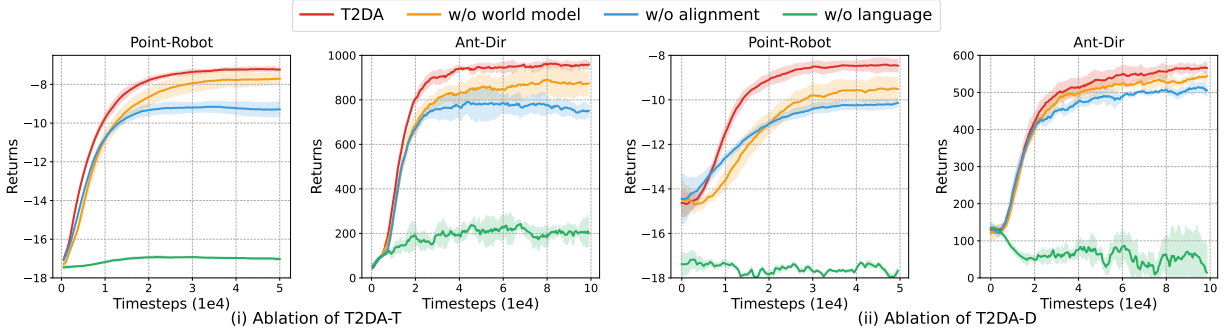


Figure 4: Ablation results on both T2DA-D and T2DA-T using Mixed datasets. *w/o world model* omits pre-training the trajectory encoder, *w/o alignment* omits contrastive pre-training, and *w/o language* omits the language supervision.

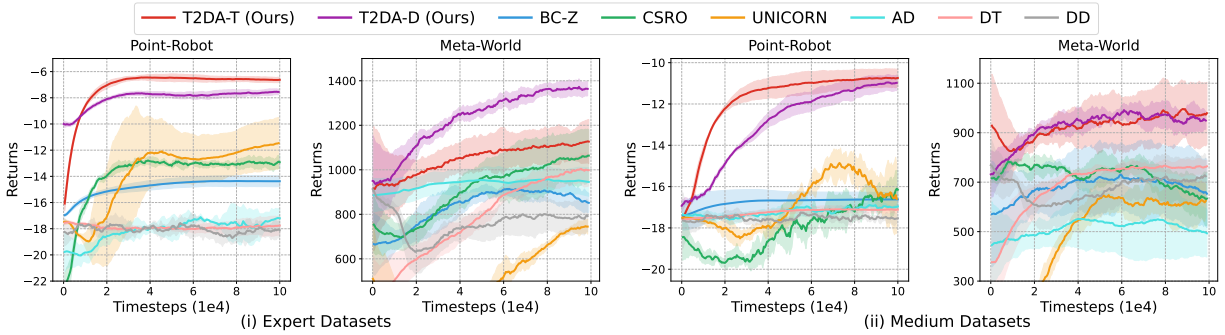


Figure 5: Results of robustness to data quality where T2DA is compared against baselines using Expert and Medium datasets. Both T2DA-D and T2DA-T achieve consistent superiority across datasets of varying quality.

ically demonstrates lower variance during generalist policy learning, signifying not only enhanced learning efficiency but also improved training stability.

4.2 Ablation Study

We compare T2DA to three ablations: 1) *w/o world model*, it eliminates pre-training the trajectory encoder and instead updates it jointly with the text encoder during contrastive pre-training; 2) *w/o alignment*, it omits contrastive language-decision pre-training and fixes the text encoder initialized from pre-trained language models; and 3) *w/o language*, it completely removes the text encoder.

Figure 4 presents ablation results of both the T2DA-D and T2DA-T architectures. First, the elimination of pre-training the trajectory encoder (T2DA *vs.* *w/o world model*) results in decreased test returns with greater variances. It indicates that capturing environment dynamics via the world model can enable more precise and stable knowledge alignment between text and decision. Second, omitting the language-decision pre-training (*w/o world model vs. w/o alignment*) further decreases the performance. It confirms the existence of a semantic gap between text and decision, whereas the gap can be effectively bridged by contrastive knowledge alignment. Finally, removing the language supervision (*w/o alignment vs. w/o language*) can produce catastrophic performance with poor zero-shot generalization, highlighting the necessity of leveraging a wealth of knowledge from natural language. In summary, the performance of T2DA declines when any component is omitted, verifying that all components are essential to its final capabilities.

4.3 Robustness Study

Robustness to Data Quality. We compare T2DA against baselines using Expert and Medium offline datasets. As shown in Figure 5, both T2DA-D and T2DA-T consistently outperform baselines on these datasets. Notably, while most baselines suffer significant performance degradation when trained on Medium datasets, T2DA maintains high-capacity generalization despite the lower data quality. It showcases the promising applicability of T2DA in real-

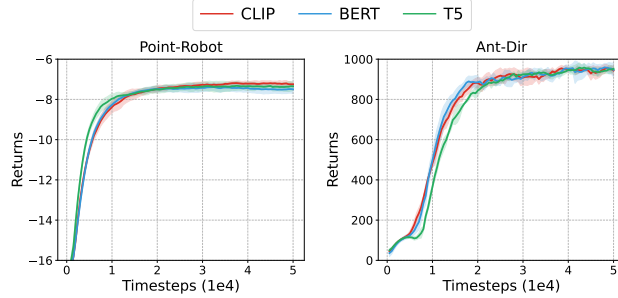


Figure 6: Results of robustness to text encoders where T2DA initializes the text encoder from CLIP, BERT, and T5, showing that T2DA can efficiently harness language knowledge embedded in different language models.

world scenarios where the agent often needs to learn from sub-optimal data. In summary, T2DA achieves consistent superiority across datasets of varying quality, yielding excellent robustness.

Robustness to Text Encoders. We also investigate T2DA’s sensitivity to different representations of language supervision by initializing the text encoder from three distinct language models: CLIP [12], BERT [49], and T5 [41]. As shown in Figure 6, the near-identical performance across all language models highlights that T2DA’s effectiveness is independent of the specific text encoder architecture. It suggests that T2DA can effectively leverage the semantic understanding capabilities inherent to different language models while maintaining consistent performance.

4.4 Visualization Insights

We gain deep insights into the knowledge alignment between text and decision through t-SNE visualization on the example Ant-Dir task as shown in Figure 1 in Sec. 1. Appendix G shows more visualization results.

Decision Embeddings. Raw embeddings are derived from a randomly initialized trajectory encoder. In the dynamics-aware embedding space, sample points from different tasks are more clearly distinguished, and similar tasks are grouped more closely. This suggests the successful capture of task-specific environment dynamics via the world model.

Text Embeddings. Raw embeddings are derived from pre-trained language models. In the aligned space, text embeddings follow a more distinguished distribution that matches the metric of task similarity, highlighting the successful bridging of the semantic gap. Notably, the aligned embeddings follow a cyclic spectrum that matches the periodicity of angular directions in a physical sense, showing efficient comprehension of the environment dynamics.

5 Conclusions, Limitations, and Future Work

In the paper, we tackle the generalization challenge in decision domains via leveraging a much broader source of supervision from natural language. Improvements in zero-shot generalization capacities highlight the potential impact of our scalable implementations: text-to-decision diffuser and text-to-decision transformer. These findings open up new avenues for building more flexible and accessible generalist agents that can understand and act upon natural language instructions without extensive domain-specific training.

Though, our agent is trained on lightweight datasets compared to popular large models. An essential step is to implement on vast datasets with diversified domains, unleashing the scaling law with the diffusion or transformer architectures. Another step is to deploy the text-to-decision paradigm on real robots toward embodied intelligence.

References

- [1] V. Mnih, K. Kavukcuoglu, D. Silver, A. A. Rusu, J. Veness *et al.*, “Human-level control through deep reinforcement learning,” *Nature*, vol. 518, no. 7540, pp. 529–533, 2015.
- [2] A. Fawzi, M. Balog, A. Huang, T. Hubert, B. Romera-Paredes *et al.*, “Discovering faster matrix multiplication algorithms with reinforcement learning,” *Nature*, vol. 610, no. 7930, pp. 47–53, 2022.
- [3] R. Rafailov, A. Sharma, E. Mitchell, C. D. Manning, S. Ermon, and C. Finn, “Direct preference optimization: Your language model is secretly a reward model,” in *Advances in Neural Information Processing Systems*, vol. 36, 2023.

- [4] K. Black, M. Janner, Y. Du, I. Kostrikov, and S. Levine, “Training diffusion models with reinforcement learning,” in *Proceedings of International Conference on Learning Representations*, 2024.
- [5] D. Guo, D. Yang, H. Zhang, J. Song, R. Zhang *et al.*, “DeepSeek-R1: Incentivizing reasoning capability in llms via reinforcement learning,” *arXiv preprint arXiv:2501.12948*, 2025.
- [6] K. Black, N. Brown, D. Driess, A. Esmail, M. Equi, C. Finn, N. Fusai, L. Groom, K. Hausman, B. Ichter *et al.*, “ π_0 : A vision-language-action flow model for general robot control,” *arXiv preprint arXiv:2410.24164*, 2024.
- [7] T. Schmied, M. Hofmarcher, F. Paischer, R. Pascanu, and S. Hochreiter, “Learning to modulate pre-trained models in RL,” in *Advances in Neural Information Processing Systems*, 2023.
- [8] M. Xu, Y. Shen, S. Zhang, Y. Lu, D. Zhao, J. Tenenbaum, and C. Gan, “Prompting decision transformer for few-shot policy generalization,” in *Proceedings of International Conference on Machine Learning*, vol. 162, 2022, pp. 24 631–24 645.
- [9] Y. Gao, R. Zhang, J. Guo, F. Wu, Q. Yi, S. Peng, S. Lan, R. Chen, Z. Du, X. Hu *et al.*, “Context shift reduction for offline meta-reinforcement learning,” in *Advances in Neural Information Processing Systems*, vol. 36, 2023.
- [10] Z. Wang, L. Zhang, W. Wu, Y. Zhu, D. Zhao, and C. Chen, “Meta-DT: Offline meta-rl as conditional sequence modeling with world model disentanglement,” in *Advances in Neural Information Processing Systems*, 2024.
- [11] J. Achiam, S. Adler, S. Agarwal, L. Ahmad, I. Akkaya *et al.*, “GPT-4 technical report,” *arXiv preprint arXiv:2303.08774*, 2023.
- [12] A. Radford, J. W. Kim, C. Hallacy, A. Ramesh, G. Goh *et al.*, “Learning transferable visual models from natural language supervision,” in *Proceedings of International Conference on Machine Learning*, 2021, pp. 8748–8763.
- [13] C. Schirmann, N. D. Singh, F. Croce, and M. Hein, “Robust CLIP: Unsupervised adversarial fine-tuning of vision embeddings for robust large vision-language models,” in *Proceedings of International Conference on Machine Learning*, 2024.
- [14] M. Ahn, A. Brohan, N. Brown, Y. Chebotar, O. Cortes, B. David, C. Finn, C. Fu, K. Gopalakrishnan, K. Hausman *et al.*, “Do as I can, not as I say: Grounding language in robotic affordances,” in *Proceedings of Conference on Robot Learning*, 2022.
- [15] Y. Zhai, H. Bai, Z. Lin, J. Pan, S. Tong, Y. Zhou, A. Suhr, S. Xie, Y. LeCun, Y. Ma *et al.*, “Fine-tuning large vision-language models as decision-making agents via reinforcement learning,” in *Advances in Neural Information Processing Systems*, 2024.
- [16] A. Szot, M. Schwarzer, H. Agrawal, B. Mazouze, R. Metcalf, W. Talbott, N. Mackraz, R. D. Hjelm, and A. T. Toshev, “Large language models as generalizable policies for embodied tasks,” in *Proceedings of International Conference on Learning Representations*, 2024.
- [17] J. Rocamonde, V. Montesinos, E. Nava, E. Perez, and D. Lindner, “Vision-language models are zero-shot reward models for reinforcement learning,” in *Proceedings of International Conference on Learning Representations*, 2024.
- [18] T. Xie, S. Zhao, C. H. Wu, Y. Liu, Q. Luo, V. Zhong, Y. Yang, and T. Yu, “Text2Reward: Reward shaping with language models for reinforcement learning,” in *Proceedings of International Conference on Learning Representations*, 2024.
- [19] E. Jang, A. Irpan, M. Khansari, D. Kappler, F. Ebert, C. Lynch, S. Levine, and C. Finn, “BC-Z: Zero-shot task generalization with robotic imitation learning,” in *Proceedings of Conference on Robot Learning*, 2022, pp. 991–1002.
- [20] J.-C. Pang, S.-H. Yang, K. Li, J. Zhang, X.-H. Chen, N. Tang, and Y. Yu, “Knowledgeable agents by offline reinforcement learning from large language model rollouts,” in *Advances in Neural Information Processing Systems*, 2024.
- [21] C. Finn, P. Abbeel, and S. Levine, “Model-agnostic meta-learning for fast adaptation of deep networks,” in *Proceedings of International conference on machine learning*, 2017, pp. 1126–1135.
- [22] E. Mitchell, R. Rafailov, X. B. Peng, S. Levine, and C. Finn, “Offline meta-reinforcement learning with advantage weighting,” in *Proceedings of International Conference on Machine Learning*, 2021, pp. 7780–7791.
- [23] K. Rakelly, A. Zhou, C. Finn, S. Levine, and D. Quillen, “Efficient off-policy meta-reinforcement learning via probabilistic context variables,” in *Proceedings of International Conference on Machine Learning*, 2019, pp. 5331–5340.
- [24] L. Zintgraf, S. Schulze, C. Lu, L. Feng, M. Igl, K. Shiarlis, Y. Gal, K. Hofmann, and S. Whiteson, “VariBAD: Variational Bayes-adaptive deep RL via meta-learning,” *The Journal of Machine Learning Research*, vol. 22, no. 1, pp. 13 198–13 236, 2021.
- [25] H. Yuan and Z. Lu, “Robust task representations for offline meta-reinforcement learning via contrastive learning,” in *Proceedings of International Conference on Machine Learning*, 2022, pp. 25 747–25 759.
- [26] L. Li, H. Zhang, X. Zhang, S. Zhu, J. Zhao, and P.-A. Heng, “Towards an information theoretic framework of context-based offline meta-reinforcement learning,” in *Advances in Neural Information Processing Systems*, 2024.
- [27] S. Huang, J. Hu, H. Chen, L. Sun, and B. Yang, “In-context decision transformer: Reinforcement learning via hierarchical chain-of-thought,” in *Proceedings of International Conference on Machine Learning*, 2024.
- [28] J. Grigsby, L. Fan, and Y. Zhu, “AMAGO: Scalable in-context reinforcement learning for adaptive agents,” in *Proceedings of International Conference on Learning Representations*, 2024.
- [29] M. Laskin, L. Wang, J. Oh, E. Parisotto, S. Spencer *et al.*, “In-context reinforcement learning with algorithm distillation,” in *Proceedings of International Conference on Learning Representations*, 2023.

- [30] J. Lee, A. Xie, A. Pacchiano, Y. Chandak, C. Finn, O. Nachum, and E. Brunskill, “Supervised pretraining can learn in-context reinforcement learning,” *Advances in Neural Information Processing Systems*, vol. 36, 2023.
- [31] R. Shi, Y. Liu, Y. Ze, S. S. Du, and H. Xu, “Unleashing the power of pre-trained language models for offline reinforcement learning,” in *Proceedings of International Conference on Learning Representations*, 2024.
- [32] T. Carta, C. Romac, T. Wolf, S. Lamprier, O. Sigaud, and P.-Y. Oudeyer, “Grounding large language models in interactive environments with online reinforcement learning,” in *Proceedings of International Conference on Machine Learning*, 2023, pp. 3676–3713.
- [33] W. Tan, W. Zhang, S. Liu, L. Zheng, X. Wang, and B. An, “True knowledge comes from practice: Aligning large language models with embodied environments via reinforcement learning,” in *Proceedings of International Conference on Learning Representations*, 2024.
- [34] M. Kwon, S. M. Xie, K. Bullard, and D. Sadigh, “Reward design with language models,” in *Proceedings of International Conference on Learning Representations*, 2023.
- [35] Y. Fu, H. Zhang, D. Wu, W. Xu, and B. Boulet, “FuRL: Visual-language models as fuzzy rewards for reinforcement learning,” in *Proceedings of International Conference on Machine Learning*, 2024.
- [36] B. Wang, Y. Qu, Y. Jiang, J. Shao, C. Liu, W. Yang, and X. Ji, “LLM-empowered state representation for reinforcement learning,” in *Proceedings of International Conference on Machine Learning*, 2024.
- [37] F. Hill, S. Mokra, N. Wong, and T. Harley, “Human instruction-following with deep reinforcement learning via transfer-learning from text,” *arXiv preprint arXiv:2005.09382*, 2020.
- [38] M. Alomari, P. Duckworth, D. Hogg, and A. Cohn, “Natural language acquisition and grounding for embodied robotic systems,” in *Proceedings of AAAI Conference on Artificial Intelligence*, vol. 31, no. 1, 2017.
- [39] A. Akakzia, C. Colas, P.-Y. Oudeyer, M. Chetouani, and O. Sigaud, “Grounding language to autonomously-acquired skills via goal generation,” in *Proceedings of International Conference on Learning Representations*, 2021.
- [40] J.-C. Pang, X.-Y. Yang, S.-H. Yang, X.-H. Chen, and Y. Yu, “Natural language instruction-following with task-related language development and translation,” in *Advances in Neural Information Processing Systems*, vol. 36, 2023.
- [41] C. Raffel, N. Shazeer, A. Roberts, K. Lee, S. Narang, M. Matena, Y. Zhou, W. Li, and P. J. Liu, “Exploring the limits of transfer learning with a unified text-to-text transformer,” *Journal of Machine Learning Research*, vol. 21, no. 140, pp. 1–67, 2020.
- [42] E. J. Hu, P. Wallis, Z. Allen-Zhu, Y. Li, S. Wang, L. Wang, W. Chen *et al.*, “LoRA: Low-rank adaptation of large language models,” in *Proceedings of International Conference on Learning Representations*, 2022.
- [43] A. Ajay, Y. Du, A. Gupta, J. Tenenbaum, T. Jaakkola, and P. Agrawal, “Is conditional generative modeling all you need for decision-making?” in *Proceedings of International Conference on Learning Representations*, 2023.
- [44] L. Chen, K. Lu, A. Rajeswaran, K. Lee, A. Grover, M. Laskin, P. Abbeel, A. Srinivas, and I. Mordatch, “Decision transformer: Reinforcement learning via sequence modeling,” in *Advances in Neural Information Processing Systems*, vol. 34, 2021, pp. 15 084–15 097.
- [45] C. Saharia, W. Chan, S. Saxena, L. Li, J. Whang *et al.*, “Photorealistic text-to-image diffusion models with deep language understanding,” in *Advances in Neural Information Processing Systems*, vol. 35, 2022, pp. 36 479–36 494.
- [46] L. Zhang, A. Rao, and M. Agrawala, “Adding conditional control to text-to-image diffusion models,” in *Proceedings of IEEE/CVF International Conference on Computer Vision*, 2023, pp. 3836–3847.
- [47] T. Haarnoja, A. Zhou, P. Abbeel, and S. Levine, “Soft actor-critic: Off-policy maximum entropy deep reinforcement learning with a stochastic actor,” in *Proceedings of International Conference on Machine Learning*, 2018, pp. 1861–1870.
- [48] J. Fu, A. Kumar, O. Nachum, G. Tucker, and S. Levine, “D4RL: Datasets for deep data-driven reinforcement learning,” *arXiv preprint arXiv:2004.07219*, 2020.
- [49] J. D. M.-W. C. Kenton and L. K. Toutanova, “BERT: Pre-training of deep bidirectional transformers for language understanding,” in *Proceedings of the North American Chapter of the Association for Computational Linguistics - Human Language Technologies*, vol. 1, no. 2, 2019.
- [50] T. Yu, D. Quillen, Z. He, R. Julian, K. Hausman, C. Finn, and S. Levine, “Meta-World: A benchmark and evaluation for multi-task and meta reinforcement learning,” in *Proceedings of Conference on Robot Learning*, 2020, pp. 1094–1100.
- [51] W. Peebles and S. Xie, “Scalable diffusion models with transformers,” in *Proceedings of the IEEE/CVF International Conference on Computer Vision*, 2023, pp. 4195–4205.
- [52] D. Hendrycks and K. Gimpel, “Gaussian error linear units (GELUS),” *arXiv preprint arXiv:1606.08415*, 2016.

A Algorithm Pseudocodes

Based on the implementations in Sec. 3, this appendix gives the brief procedures of each component in T2DA. First, Algorithm 1 presents the pre-training of the generalized world model. Based on the dynamics-aware decision embedding encoded by Algorithm 1, Algorithm 2 shows the contrastive language-decision pre-training that bridges the semantic gap between text and decision, and aligns text embeddings to comprehend the environment dynamics of decision tasks.

Then, Algorithm 3 and Algorithm 4 present the model training processes of Text-to-Decision Diffuser and Text-to-Decision Transformer, respectively, where the generalist policy is conditioned on the text embeddings fine-tuned in Algorithm 2. Finally, Algorithm 5 and Algorithm 6 show zero-shot evaluations on test tasks, where the agent can directly realize text-to-decision generation according to textual instructions at hand.

Algorithm 1: Pre-training the generalized world model

Input: Offline datasets $\mathcal{D}_{\text{train}}$; Batch size m
Trajectory encoder ϕ ; Reward decoder \mathcal{R}_φ and Transition decoder \mathcal{T}_φ

- 1 **for** each iteration **do**
- 2 **for** $i = 1, \dots, m$ **do**
- 3 Sample a task M_k and obtain the corresponding dataset \mathcal{D}_k from $\mathcal{D}_{\text{train}}$
- 4 Sample two trajectories from \mathcal{D}_k as $\tau = (s_0, a_0, r_0, s_1, a_1, r_1, \dots)$ and $\tau^* = (s_0^*, a_0^*, r_0^*, s_1^*, a_1^*, r_1^*, \dots)$
- 5 Obtain the decision embedding by feeding τ to the trajectory encoder as $z = \phi(\tau)$
- 6 **for** $t = 0, 1, \dots$ **do**
- 7 Compute the predicted reward $\hat{r}_t^* = \mathcal{R}_\varphi(s_t^*, a_t^*; z)$ and next state $\hat{s}_{t+1}^* = \mathcal{T}_\varphi(s_t^*, a_t^*; z)$ on trajectory τ^*
- 8 **end**
- 9 **end**
- 10 Update ϕ and φ jointly using loss $\mathcal{L}(\phi, \varphi) = \frac{1}{m} \sum_i \sum_t \left[(r_t^* - \mathcal{R}_\phi(s_t^*, a_t^*; z))^2 + (s_{t+1}^* - \mathcal{T}_\varphi(s_t^*, a_t^*; z))^2 \right]$
- 11 **end**

Algorithm 2: Contrastive Language-Decision Pre-training

Input: Offline datasets $\mathcal{D}_{\text{train}}$; Batch size N
Pre-trained trajectory encoder ϕ ; Text encoder ψ

- 1 Freeze the trajectory encoder ϕ pre-trained in Algorithm 1
- 2 Initialize text encoder ψ from popular pre-trained language models like CLIP or T5
- 3 **for** each iteration **do**
- 4 Sample a batch of N (trajectory τ , textual task description l) pairs from $\mathcal{D}_{\text{train}}$
- 5 Compute the symmetric similarities between the two modalities, $\text{sim}(\tau, l)$ and $\text{sim}(l, \tau)$, as in Eq. (4)
- 6 Derive the decision-to-text and text-to-decision similarity scores, $p(\tau)$ and $p(l)$, as in Eq. (5)
- 7 Update the text encoder ψ using LoRA by minimizing the symmetric cross-entropy loss $\mathcal{L}(\psi)$ as in Eq. (6)
- 8 **end**

Algorithm 3: Model Training of Text-to-Decision Diffuser

Input: Offline datasets $\mathcal{D}_{\text{train}} = \sum_k (\mathcal{D}_k, l_k)$; Pre-trained text encoder ψ
Noise model ϵ_θ ; Batch size N

- 1 Freeze the text encoder ψ pre-trained in Algorithm 2
- 2 **while** not converged **do**
- 3 Sample a batch of N (trajectory $x_0(\tau^k)$, language supervision l_k) pairs from different tasks in $\mathcal{D}_{\text{train}}$
- 4 $c \sim \text{Uniform}(\{1, \dots, C\})$
- 5 $\epsilon \sim \mathcal{N}(0, I)$
- 6 $x_c(\tau_{s_t}^k) \leftarrow s_t^k$ // Constrain the first state of the plan
- 7 Take gradient descent step on $\nabla_\theta \sum_{k=1}^N \left\| \epsilon - \epsilon_\theta \left(x_c(\tau^k), \hat{R}(\tau), \psi(l_k), c \right) \right\|^2$
- 8 **end**

Algorithm 4: Model Training of Text-to-Decision Transformer

Input: Offline datasets $\mathcal{D}_{\text{train}} = \sum_k (\mathcal{D}_k, l_k)$; Pre-trained text encoder ψ
 Causal transformer F_θ ; Batch size N

- 1 Freeze the text encoder ψ pre-trained in Algorithm 2
- 2 **while** *not converged* **do**
- 3 Sample a batch of N (trajectory τ_k , language supervision l_k) pairs from different tasks in $\mathcal{D}_{\text{train}}$
- 4 Get a batch of inputs $\mathcal{B} = \{\tau_k^+\}_{k=1}^N$, where $\tau_k^+ = (\psi(l_k), \hat{R}_{t-H+1}^k, s_{t-H+1}^k, a_{t-H+1}^k, \dots, \hat{R}_t^k, s_t^k, a_t^k)$
- 5 $a^{\text{pred}} = F_\theta(\tau_k^+), \forall \tau_k^+ \in \mathcal{B}$
- 6 Minimize loss $\mathcal{L}(\theta) = \frac{1}{N} \sum_{\tau_k^+ \in \mathcal{B}} (a - a^{\text{pred}})^2$
- 7 **end**

Algorithm 5: Zero-Shot Evaluation of Text-to-Decision Diffuser

Input: Language instruction l_{new} ; Pre-trained text encoder ψ
 Trained noise model ϵ_θ ; Diffusion steps C ; Guidance scale w

- 1 Obtain the text embedding from language instruction as $\psi(l_{\text{new}})$
- 2 **while** *not done* **do**
- 3 Observe state s_t ; Initialize $x_c(\tau) \sim \mathcal{N}(0, \alpha I)$
- 4 **for** $c = C, \dots, 1$ **do**
- 5 $x_c(\tau_{s_t}) \leftarrow s_t$ // Constrain the first state of the plan
- 6 $\hat{\epsilon} \leftarrow \epsilon_\theta(x_c(\tau), c) + w [\epsilon_\theta(x_c(\tau), \hat{R}(\tau), \psi(l_{\text{new}}), c) - \epsilon_\theta(x_c(\tau), c)]$ // Classifier-free guidance
- 7 $(\mu_{c-1}, \Sigma_{c-1}) \leftarrow \text{Denoise}(x_c(\tau), \hat{\epsilon})$
- 8 $x_{c-1}(\tau) \sim \mathcal{N}(\mu_{c-1}, \alpha \Sigma_{c-1})$
- 9 **end**
- 10 Execute first action of plan as $a_t \leftarrow x_0(\tau_{a_t})$
- 11 $t \leftarrow t + 1$
- 12 **end**

Algorithm 6: Zero-Shot Evaluation of Text-to-Decision Transformer

Input: Language instruction l_{new} ; Pre-trained text encoder ψ
 Trained casual transformer F_θ ; Target return G^*

- 1 Obtain the text embedding from language instruction as $\psi(l_{\text{new}})$
- 2 Initialize desired return $\hat{R} = G^*$
- 3 **for each timestep** t **do**
- 4 Observe state s_t
- 5 Obtain the H -step history trajectory as $\tau = (\hat{R}_{t-H+1}, s_{t-H+1}, a_{t-H+1}, \dots, \hat{R}_t, s_t)$
- 6 Augment the trajectory with the text embedding as $\tau^+ = (\psi(l_{\text{new}}), \tau)$
- 7 Get action $a_t = F_\theta(\tau^+)$
- 8 Step env. and get feedback $s, a, r, \hat{R} \leftarrow \hat{R} - r$
- 9 Append (\hat{R}, s, a) to recent history τ
- 10 **end**

B Evaluation Environments and Dataset Construction

B.1 The Details of Environments

We evaluate T2DA and all the baselines on three classical benchmarks that are widely adopted to assess the generalization capacity of RL algorithms, containing the following four environments:

- **Point-Robot** is a 2D navigation environment where an agent starts from a fixed origin and navigates to a target location g . The agent receives its coordinate position as the observation and outputs actions in the range of $[-0.1, 0.1]^2$, representing displacement in the X - and Y -axis directions. The reward is the negative Euclidean distance to the goal: $r_t = -\|s_t - g\|_2$,

where s_t denotes the current position. The maximal episode step is set to 20. Tasks differ in the target location g that is randomly sampled within a unit square of $[-0.5, 0.5]^2$. Each task is captioned by a text description as “Please navigate to the goal position of g ”.

- **Cheetah-Vel** is a multi-task MuJoCo environment where a planar cheetah robot aims to run a target velocity v_g along the X -axis. The reward function combines a quadratic control cost and a velocity matching term as $r_t = -0.05\|a_t\|_2 - |v_t - v_g|$, where a_t and v_t represent the action and current velocity, respectively. The maximal episode step is set to 200. Tasks differ in the target velocity v_g that is randomly sampled from a uniform distribution as $v_g \sim \text{Uniform}[0.075, 3.0]$. Each task is captioned by a text description as “Please run at the target velocity of v_g ”.
- **Ant-Dir** is also a multi-task MuJoCo environment where a 3D ant robot navigates toward a target direction θ . The primary reward component measures directional alignment as $r_{\text{forward}} = v_x \cos \theta + v_y \sin \theta$, where (v_x, v_y) represents the horizontal and vertical velocities. The final reward incorporates additional terms for the control cost, contact penalty, and survival bonus. The maximal episode step is set to 200. Tasks differ in the goal direction θ that is uniformly sampled from the full space as $\theta \sim \text{Uniform}[0, 2\pi]$. Each task is captioned by a text description as “Please walk toward the target direction of θ ”.
- **Meta-World** comprises 50 robotic manipulation tasks where a robotic arm interacts with various objects on a tabletop. Each task’s reward function (ranging from 0 to 10) combines multiple components for fundamental behaviors (such as reaching, grasping, and placing), with 10 indicating successful completion. The maximal episode step is set to 200. Table 2 illustrates the detailed description of the training and test tasks. More details can be found in [50].

For each domain of Point-Robot, Cheetah-Vel, and Ant-Dir, we sample 50 tasks in total and split them into 45 training tasks and 5 test tasks. For Meta-World, we use 18 training tasks and 4 test tasks as detailed as shown in Table 2.

Table 2: Details of the training and test tasks of Meta-World.

Training Task	Description
faucet-close	rotate faucet clockwise
door-lock	lock door by rotating clockwise
door-unlock	unlock door by rotating counter-clockwise
window-close	push and close window
window-open	push and open window
coffee-button	push button on coffee machine
drawer-open	open drawer
door-open	open door with revolving joint
button-press	press button
button-press-topdown	press button from top
button-press-topdown-wall	bypass wall and press button from top
button-press-wall	bypass wall and press button
handle-press	press handle down
handle-pull	pull handle up
plate-slide-back	slide plate back
plate-slide-side	slide plate side
plate-slide	slide plate
plate-slide-back-side	slide plate back side
Test Task	Description
faucet-open	rotate faucet counter-clockwise
drawer-close	push and close drawer
reach-wall	bypass wall and reach goal
handle-press-side	press handle down sideways

B.2 The Details of Datasets

We employ the soft actor-critic (SAC) algorithm [47] to independently train a policy for each task and save policy checkpoints at different training steps. The hyperparameters used for SAC training across all environments are listed in Table 3. We consider three types of datasets as

- **Medium:** We load the checkpoint of a medium policy that achieves approximately half the performance of expert policies, and use the medium policy to generate a number of trajectories to construct the Medium dataset.
- **Expert:** We load the checkpoint of an expert policy that achieves the highest return after the convergence of training, and use the expert policy to collect several trajectories to construct the Expert dataset.

- **Mixed:** We load all saved checkpoints of policies at different training steps, and use these policies to generate a diverse set of trajectories to construct the Mixed dataset.

Specifically, we collect 200 trajectories for each kind of dataset in all evaluated environments.

Table 3: Hyperparameters of SAC used to collect multi-task offline datasets.

Environments	Training steps	Warmup steps	Save frequency	Learning rate	Soft update	Discount factor	Entropy ratio
Point-Robot	2000	100	40	3e-4	0.005	0.99	0.2
Cheetah-Vel	500000	2000	10000	3e-4	0.005	0.99	0.2
Ant-Dir	500000	2000	10000	3e-4	0.005	0.99	0.2
Meta-World	1000000	5000	100	1e-3	0.005	0.99	0.2

C Baseline Methods

This section gives details of the competitive baselines, including context-based offline meta-RL (OMRL), in-context RL, and language-conditioned policy learning approaches. These baselines are thoughtfully selected to cover the main studies that tackle the generalization problem of RL algorithms. The baselines are introduced as follows:

- **CSRO** [9], **Context Shift Reduction for OMRL**. It addresses the context shift problem in offline meta-RL through two key components: 1) During meta-training, it employs a max-min mutual information representation learning mechanism to minimize mutual information between the task representation and the behavior policy while maximizing mutual information between the task representation and the task information; 2) During meta-test, it introduces a non-prior context collection strategy to first randomly explore the environment and then gradually update the task representation.
- **UNICORN** [26], **Unified Information Theoretic Framework of Context-Based Offline Meta-Reinforcement Learning**. It provides a general framework to unify several context-based offline meta-RL algorithms by proving that they optimize different bounds of mutual information between the task variable M and latent representation Z . Based on this theoretical insight, it proposes a supervised and a self-supervised implementation of the mutual information derivation $I(Z; M)$.
- **AD** [29], **Algorithm Distillation**. It distills RL algorithms into neural networks by modeling their training histories with a causal sequence model. Using a dataset of learning histories generated by a source RL algorithm, AD trains a causal transformer to autoregressively predict actions given their preceding learning histories as the context, enabling in-context policy improvement without updating network parameters.
- **BC-Z** [19], **Behavior Cloning Z**. It is an imitation learning system designed for zero-shot generalization to novel vision-based manipulation tasks. It flexibly conditions the policy on pre-trained embeddings of natural language or video of human-performing tasks. To align BC-Z to the benchmarks investigated in this paper, we replace the video data with RL datasets $\mathcal{D} = \sum_i (s_i, a_i, r_i, s'_i)$ and modify its video encoder to a trajectory encoder ϕ identical to that used in T2DA. This adjustment for a fair comparison results in the optimization objective: $\min_{\sum_{\text{task } k} \sum_{(s, a) \sim \mathcal{D}} [-\log \pi(a|s, \psi(l_k)) + D_{\cos}(\psi(l_k), \phi(\tau_k))]$, where D_{\cos} denotes the cosine distance.
- **DD** [43], **Decision Diffuser**. It is a conditional generative modeling framework that reformulates offline decision-making through diffusion models. It reformulates RL by: 1) Modeling policies as return-conditional diffusion models that generate state trajectories; 2) Using classifier-free guidance with low-temperature sampling to extract high-quality behaviors from offline datasets; 3) Supporting flexible composition of multiple constraints or skills at test time by combining their respective noise prediction models.
- **DT** [44], **Decision Transformer**. It is a framework that reformulates RL as sequence modeling through the transformer architecture. It has two key components: 1) Casting the RL problem as conditional sequence modeling where the model learns to generate actions by conditioning on returns and past states and actions; 2) Using a causally masked transformer architecture that enables direct credit assignment through self-attention mechanisms.

For a fair comparison, all baselines are adjusted to an aligned zero-shot setting, where no warm-start data is available before policy evaluation. All these baselines can only use samples generated by the trained meta-policy during evaluation to infer task representations.

D Network Architecture and Hyperparameters of T2DA

This appendix gives details of the architecture and hyperparameters of T2DA implementations as follows.

- **World Model**. We implement the generalized world model using simple architecture: a trajectory encoder and two decoders for the reward and state transition prediction. Specifically, the trajectory encoder consists of a transformer encoder with 6 layers,

where each layer contains a multi-head self-attention module (8 heads) and a feed-forward network with ReLU activation. States, actions, and rewards in the raw trajectory are first tokenized into 256-dimensional vectors through separate linear layers. These embeddings are concatenated and processed by the transformer encoder to produce a 256-dimensional decision embedding z via mean pooling and linear projection. Two MLPs serve as decoders: a reward decoder that predicts the instant reward r given the tuple $(s, a, s'; z)$, and a state transition decoder that predicts the next state s' given the tuple $(s, a, r; z)$. Both MLPs utilize two hidden layers of 256 dimensions each.

- **Text Encoder.** We initialize text encoders from pre-trained CLIP [12], BERT [49], and T5 [41] in this paper. Specifically, we use `openai/clip-vit-base-patch32`, `google-bert/bert-base-uncased`, and `google-t5/t5-small`, respectively.
- **Diffusion Architecture of T2DA.** We implement the diffusion architecture of T2DA-D based on the decision diffuser [43] framework². Following DiT [51], we replace U-Net backbone with a transformer to represent the noise model ϵ_θ . Each block employs a multi-head self-attention module followed by a feed-forward network with GELU activation [52], using adaptive layer normalization (adaLN) for conditioning. The model processes state-action trajectories through linear embeddings, which are combined with positional embeddings derived from RL timesteps. The diffusion time embeddings are encoded via sinusoidal embeddings processed through an MLP. For conditioning, text embeddings and returns-to-go are concatenated with diffusion time embeddings. The detailed configurations and hyperparameters of T2DA-D are presented in Table 5.
- **Transformer Architecture of T2DA.** We implement the transformer architecture of T2DA-T based on the decision transformer [44] framework³. Specifically, we employ modality-specific embeddings for states, actions, returns-to-go, and timesteps. The timestep embeddings serve as positional encodings and are added to each token embedding. These tokens are concatenated with text embedding of task description and fed into a GPT architecture which predicts actions autoregressively using a causal self-attention mask. The detailed configurations and hyperparameters of T2DA-T are presented in Table 4.

Table 4: Configurations and hyperparameters in the training process of T2DA-T.

Configuration	Point-Robot	Cheetah-Vel	Ant-Dir	Meta-World
layers num	3	3	3	3
attention head num	1	1	1	1
embedding dim	128	128	128	128
horizon	20	200	40	50
training steps	100000	70000	100000	100000
learning rate	1e-4	2e-4	1e-4	1e-4

Table 5: Configurations and hyperparameters in the training process of T2DA-D.

Configuration	Point-Robot	Cheetah-Vel	Ant-Dir	Meta-World
DiT layers num	4	4	8	4
DiT attention head num	8	8	8	8
embedding dim	128	128	256	128
horizon	10	50	40	50
diffusion steps	20	20	20	20
training steps	100000	70000	100000	100000
learning rate	5e-5	1e-4	1e-4	1e-4

E Tabular Results for Studies of Ablation, Robustness

The results for ablation and robustness studies are presented in Table 6 and Table 7, respectively.

F Analysis of Parameter-Efficient Fine-tuning

As stated in Sec. 3.3, we employ LoRA, a classical parameter-efficient fine-tuning method, to fine-tune the text encoder at a lightweight cost. As shown in Table 8, the number of trainable parameters is substantially smaller than full-parameter fine-tuning (less than 1%), enabling much more efficient computation and memory usage. To investigate whether a limited number of trainable parameters constrains the capacity for knowledge alignment, we evaluate T2DA’s performance by comparing LoRA fine-tuning

²<https://github.com/anuragajay/decision-diffuser>

³<https://github.com/kzl/decision-transformer>

Table 6: Numerical results of ablation study on both T2DA-D and T2DA-T using Mixed datasets, i.e., the final test returns after learning convergence from Figure 4. w/o world model eliminates pre-training the trajectory encoder, w/o alignment omits contrastive pre-training, and w/o language removes the language supervision. Best results in **bold**.

Environment	T2DA-T	w/o world model	w/o alignment	w/o language	T2DA-D	w/o world model	w/o alignment	w/o language
Point-Robot	-7.2 ± 0.1	-7.7 ± 0.3	-9.2 ± 0.2	-16.9 ± 0.1	-8.4 ± 0.3	-9.5 ± 0.4	-10.1 ± 0.2	-17.2 ± 0.4
Ant-Dir	963.4 ± 15.3	891.0 ± 54.4	792.3 ± 48.3	242.6 ± 13.7	568.0 ± 10.8	544.1 ± 11.1	513.8 ± 11.0	135.1 ± 10.3

Table 7: Numerical results of robustness to data quality where T2DA is compared against baselines using Expert and Medium datasets, i.e., the final test returns after learning convergence from Figure 5. Both T2DA-D and T2DA-T achieve consistent superiority across datasets of varying quality. Best results in **bold** and second best underlined.

Expert	T2DA-T	T2DA-D	BC-Z	CSRO	UNICORN	AD	DD	DT
Point-Robot	-6.4 ± 0.2	-7.5 ± 0.2	-14.4 ± 0.4	-12.8 ± 0.2	-11.5 ± 1.7	-17.1 ± 0.2	-17.6 ± 0.6	-17.5 ± 0.1
Meta-World	<u>1142.8 ± 106.6</u>	1387.7 ± 21.6	935.5 ± 26.7	1087.0 ± 78.8	787.1 ± 16.0	991.0 ± 37.7	913.4 ± 5.7	1026.0 ± 60.8
Medium	T2DA-T	T2DA-D	BC-Z	CSRO	UNICORN	AD	DD	DT
Point-Robot	-10.7 ± 0.4	-11.0 ± 0.3	-16.6 ± 0.2	-16.1 ± 0.8	-14.9 ± 0.5	-16.9 ± 0.2	-17.2 ± 0.1	-17.1 ± 0.1
Meta-World	1033.3 ± 130.6	<u>1025.3 ± 43.6</u>	756.9 ± 103.4	854.1 ± 17.9	715.8 ± 93.5	585.7 ± 126.1	768.7 ± 95.1	780.4 ± 40.8

with full-parameter fine-tuning during contrastive language-decision pre-training. Figure 7 illustrates the results on representative environments with the text encoder initialized from CLIP. Obviously, the two fine-tuning approaches yield nearly identical performance, highlighting T2DA’s superior parameter efficiency of T2DA without sacrificing effectiveness.

Table 8: The number and memory usage of parameters for LoRA fine-tuning and full-parameter fine-tuning.

Method	Trainable parameters (Memory)	Total parameters (Memory)	Percentage
LoRA Tuning	589,824 (2.25MB)	63,755,776 (243.21MB)	0.93%
Full Tuning	63,165,952 (240.96MB)	63,165,952 (240.96MB)	100%

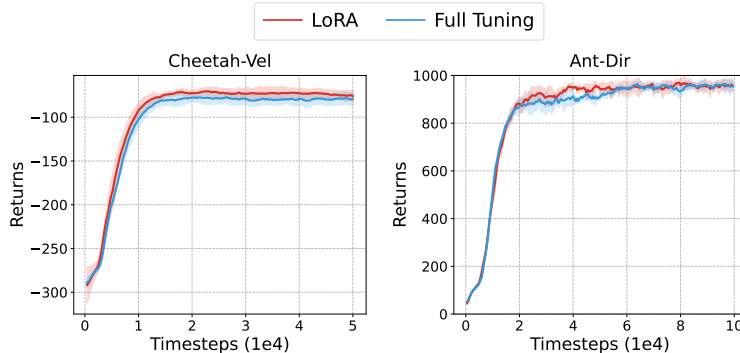


Figure 7: Test return curves of T2DA using LoRA-tuned and fully-tuned CLIP text encoders. With less than 1% parameter count, T2DA using LoRA fine-tuning yields nearly identical performance compared to full-parameter fine-tuning, highlighting T2DA’s superior parameter efficiency without sacrificing effectiveness.

G More Visualization Insights

We also visualize text and decision embeddings of the Cheetah-Vel environment through t-SNE, as shown in Figure 8.

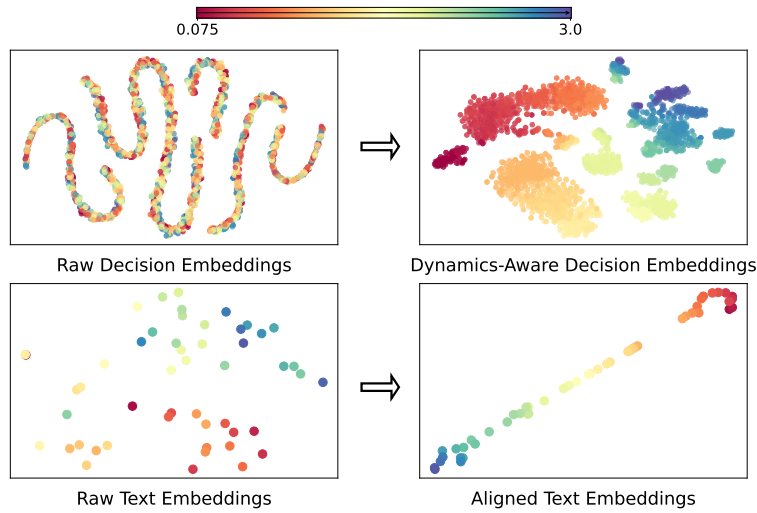


Figure 8: t-SNE visualization of Cheetah-Vel where tasks with target velocities in $[0.075, 3.0]$ are mapped into rainbow-colored points. Top: the evolution from Raw Decision Embeddings to Dynamics-Aware Decision Embeddings, where the initially entangled trajectories are transformed into well-separated clusters that highlight the successful capture of task-specific environment dynamics. Bottom: using dynamics-aware decision embeddings to align text embeddings with contrastive loss. Raw Text Embeddings are scattered with a vague distribution structure. In contrast, Aligned Text Embeddings form a clear rectilinear distribution from red (low velocity) to blue (high velocity), exactly matching the rectilinear spectrum of target velocities *in a physical sense*. This inspiring finding verifies the effective alignment of text embeddings to comprehend environment dynamics and interpretable language grounding in decision domains.